Signatures of three-dimensional photoinduced superconductivity in $YBa_2Cu_3O_{6.48}$

M. Rosenberg [1,*] D. Nicoletti [1,†] M. Buzzi [1] A. Iudica [1,2] C. Putzke,[1] Y. Liu [3] B. Keimer,[3] and A. Cavalleri [1,4,‡]

[1]*Max Planck Institute for the Structure and Dynamics of Matter, 22761 Hamburg, Germany*

[2]*Physics Department, Politecnico di Milano, 20133 Milan, Italy*

[3]*Max Planck Institute for Solid State Research, 70569 Stuttgart, Germany*

[4]*Department of Physics, Clarendon Laboratory, University of Oxford, Oxford OX1 3PU, United Kingdom*

(Received 5 June 2025; revised 29 September 2025; accepted 3 December 2025; published 30 December 2025)

Optical excitation of large-amplitude apical oxygen phonon oscillations has been shown to renormalize the electronic properties of $YBa_2Cu_3O_{6+x}$, inducing a superconducting-like optical response above equilibrium T_C. All of the evidence collected so far has been based on the changes of the terahertz frequency c-axis response. In these measurements, the capacitive interlayer coupling was seen to transform into a superconducting-like inductive response. This assignment was strengthened by recent measurements of ultrafast magnetic field expulsion. Here, we report an experimental determination of the transient in-plane optical properties, which has so far been elusive due to the high equilibrium reflectivity and the need to evaluate minute changes in the optical response. We report the appearance of a photoinduced in-plane optical gap $2\Delta \simeq 30$ cm^{-1} and a divergent imaginary conductivity, both consistent with photoinduced superconductivity. A global fit to these data suggests that in- and out-of-plane electronic properties never completely equilibrate during the dynamics.

DOI: 10.1103/2m3d-s3j9

I. INTRODUCTION

When cooled below the superconducting transition temperature, high-T_C cuprates exhibit a characteristic terahertz-frequency optical response, reflecting coherent interlayer transport and condensation of normal state quasiparticles [1–4]. A representative set of optical properties is displayed in Figs. 1(a) and 1(b), where we show the complex optical conductivity of underdoped $YBa_2Cu_3O_{6+x}$ along the c (out-of-plane) axis, for $T \gtrsim T_C$ (red) and $T \ll T_C$ (blue).

In the normal state, the real part of the optical conductivity, $\sigma_1(\omega)$, exhibits a flat and featureless spectrum below $\omega \simeq 100$ cm^{-1} [Fig. 1(a)]. At higher frequencies a collection of absorption peaks is observed, assigned to infrared-active phonons, along with a broader contribution around 400 cm^{-1}, attributed to the so-called "transverse Josephson plasmon" [5–8]. For $T < T_C$, a depletion in $\sigma_1(\omega)$ occurs and the spectral weight condenses into a zero-frequency pole, indicative of dissipationless transport. This is reflected in the imaginary part of the optical conductivity, $\sigma_2(\omega)$, as a $1/\omega$ divergence at low frequency [Fig. 1(b)], which allows the determination of the superfluid density from finite frequency measurements, as $\lim_{\omega\to 0} \omega\sigma_2(\omega) = \frac{n_S e^2}{m}$ (here n_S is the superfluid density, e the electron charge, and m the electron mass).

In a series of recent experiments, femtosecond midinfrared pulses have been used to resonantly excite apical oxygen phonon modes in underdoped $YBa_2Cu_3O_{6+x}$ [9–16]. These studies revealed a light-induced transient optical response featuring signatures of a finite superfluid density along the out-of-plane direction, as seen most directly in the transient c axis $\sigma_2(\omega)$, which acquired the same $1/\omega$ behavior observed below T_C [9,10,14–16]. Remarkably, this photoinduced response was observed all the way up to the pseudogap temperature, T^* [10,14,15]. Representative results are reported in Figs. 1(c) and 1(d), where we show the complex optical conductivity of $YBa_2Cu_3O_{6.48}$ measured at $T = 100$ K $\simeq 2T_C$ before (red) and after (blue) midinfrared photoexcitation (here, the region covered by the pump spectrum is shaded in blue) [16]. However, this analogy did not apply to the real part of optical conductivity. In the transient state, the insulating low-frequency $\sigma_1(\omega)$ showed an increase [Fig. 1(c)], as opposed to a decrease upon cooling [Fig. 1(a)]. This response could be reproduced by fitting the data with a two-fluid model, in which a superconducting term coexisted with an overdamped Drude absorption accounting for hot and incoherent normal carriers [15–19].

In a recent work [16], both the enhancement of the superfluid density, $\omega\sigma_2(\omega)$, and the dissipative response of quasiparticles, $\sigma_1(\omega)$, were investigated by systematically tuning the duration and energy of the midinfrared pump pulses, while keeping their peak field fixed. It was shown that the lifetime of the superconducting-like response coincided with the duration of the excitation pulse, up to at least $\tau \simeq 4$ ps. This allowed for a determination of well-defined optical properties over the entire probed range (as $1/\tau \simeq 0.25$ THz), removing potential ambiguities in their low-frequency limit. It was also found that the photoinduced superfluid density reached values compatible with the zero-temperature equilibrium value for

*Contact author: maor.rosenberg@mpsd.mpg.de

†Contact author: daniele.nicoletti@mpsd.mpg.de

‡Contact author: andrea.cavalleri@mpsd.mpg.de

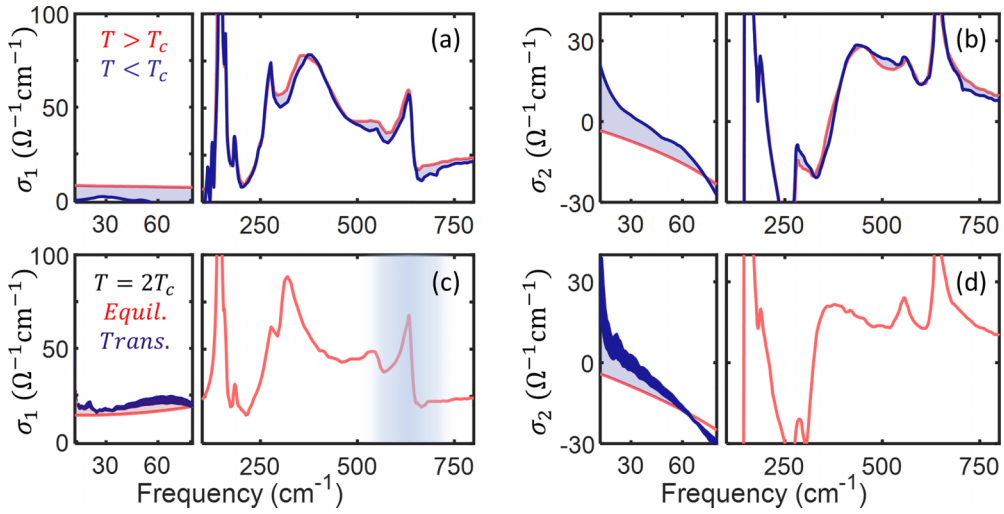

FIG. 1. (a), (b) Complex c-axis optical conductivity, $\sigma_1(\omega) + i\sigma_2(\omega)$, of underdoped $YBa_2Cu_3O_{6+x}$ across the equilibrium superconducting transition. Data at $T = 60$ K $> T_C$ (red) and $T = 10$ K $< T_C = 55$ K (blue) are reported [2,3,10,16]. Shaded blue regions represent the changes in the spectra across T_C. (c), (d) Same quantities as in (a) and (b) measured in $YBa_2Cu_3O_{6.48}$ at $T = 100$ K $\simeq 2T_C$ before (red) and after (blue) photoexcitation with ∼0.3-ps-long midinfrared pulses with a fluence of ∼8 mJ/cm^2. Red and blue areas in (c) and (d) represent photoinduced changes in the spectra, while the blue shading around 600 cm^{-1} in (c) refers to the frequency range covered by the midinfrared pump. The thickness of the blue lines indicates the uncertainty associated with the specific choice of model to deal with the pump-probe penetration depth mismatch [32].

pulses made longer than the phonon dephasing time, while the dissipative component continued to grow with increasing pulse duration. An optimal regime of pump pulse durations was identified, for which the superconducting response was maximum and that of hot quasiparticles was minimized.

Overall, this series of experiments yielded a comprehensive picture for the out-of-plane superconducting-like optical response of photoexcited $YBa_2Cu_3O_{6+x}$, addressing in detail its dependence on doping, temperature, drive duration, and photon energy. These results were also complemented by the recent discovery of a transient Meissner-like magnetic field expulsion under the same excitation conditions [20], as well as by work with second-harmonic probes that associated optically driven superconductivity in $YBa_2Cu_3O_{6.48}$ with a parametric excitation of Josephson plasmons, which are overdamped above T_C but would be made coherent by the phonon drive [21–23].

Nevertheless, a number of issues remain debated [24,25]. In the experiments discussed above, the penetration depth of the midinfrared pump (≈1 μm) was always shorter than that of the terahertz probe (5–10 μm). This mismatch was taken into account by modeling the sample as a multilayered photoexcited stack on top of an unperturbed bulk in order to obtain the optical response functions corresponding to an effective semi-infinite and homogeneously excited medium. This approach implies that, as the pump penetrates the material, its intensity is reduced and induces progressively weaker changes in the refractive index of the sample. However, for a given exponential decay of the pump intensity in the material depth, different refractive index decay profiles are possible, depending on the scaling of the pump-probe response with excitation fluence. Models with linear, square-root dependence, or assuming a saturation profile were analyzed [26,27], all returning qualitatively similar changes in transient optical properties, although different in amplitude. In Figs. 1(c) and 1(d) we show the uncertainty associated with the specific choice of model as line thickness in $\sigma_1(\omega)$ and $\sigma_2(\omega)$. It becomes evident that the superconducting-like character of the response is preserved.

Another open issue concerns the optical response measured along the Cu-O layers. If the interlayer optical conductivity is compatible with dissipationless transport [16] and magneto-optical measurements return indications of a transient Meissner effect [20], one should also expect a superconducting-like response for probe light polarized along the planes. This was not reported so far for underdoped $YBa_2Cu_3O_{6+x}$. Transient in-plane optical properties have been difficult to measure because of the high equilibrium reflectivity, from which small changes in the optical response determine the transient conductivity. Recent experiments in $La_{2-x}Ba_xCuO_4$, which reported a Josephson-like transient interlayer response for near-infrared optical excitation, did not detect any superconducting-like features in the in-plane response [28]. Yet in this work excitation was achieved with near-infrared pulses, which likely resulted in a sufficient nonequilibrium quasiparticle density to mask any sign of transient gapping. Measurements of the in-plane dynamics after excitation with optimized, midinfrared optical pulses have so far been missing.

Here, we discuss an investigation of the transient optical response of apical-oxygen-driven $YBa_2Cu_3O_{6.48}$ at terahertz frequencies along the direction parallel to the Cu-O layers. We report complex optical conductivities upon photoexcitation *qualitatively* compatible with transient superconductivity. However, unlike in the case of out-of-plane probing, the in-plane properties are *quantitatively* different from those found when cooling below T_C at equilibrium. We also propose a global fitting of these three-dimensional superconducting-like

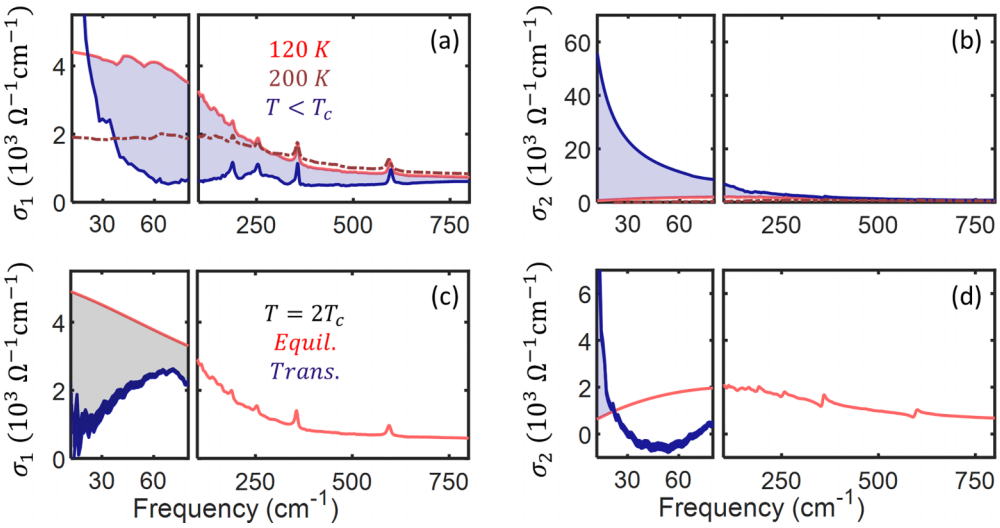

FIG. 2. (a), (b) Complex a-axis optical conductivity, $\sigma_1(\omega) + i\sigma_2(\omega)$, of underdoped $YBa_2Cu_3O_{6+x}$ across the equilibrium superconducting transition. Data at $T = 120$ K, $200\ \text{K} > T_C$ (red) and $T = 10\ \text{K} < T_C = 55$ K (blue) are plotted [29]. Shaded blue regions represent the changes in the spectra across T_C. (c), (d) Same quantities as in (a) and (b) measured in $YBa_2Cu_3O_{6.48}$ at $T = 100\ \text{K} \simeq 2T_C$ before (red) and after (blue) photoexcitation with $\sim$0.3-ps-long midinfrared pulses with a fluence of $\sim 8\ \text{mJ/cm}^2$. Shaded areas in (c) and (d) highlight the photoinduced gapping in $\sigma_1(\omega)$ and low-frequency divergence in $\sigma_2(\omega)$. The thickness of the blue lines indicates the uncertainty associated with the specific choice of model to extract the transient optical properties [32].

responses. While the reliability of our fit is not completely certain, it suggests that the in-plane and out-of-plane quasiparticle and superfluid dynamics never equilibrate.

II. EXPERIMENT

The equilibrium optical response of a single crystal of $YBa_2Cu_3O_{6.48}$ was determined with a Fourier transform infrared spectrometer. The absolute reflectivity was measured for reference at $T = 100$ K in quasi-normal-incidence geometry along the a crystallographic axes in the $\approx$15–800 cm^{-1} range with the gold evaporation technique. By using literature data [29–31] for the higher frequency range, we could perform Kramers-Kronig transformations and retrieve the complex optical conductivity (see Supplemental Material [32] for more details and Ref. [33] for source data).

Another crystal from the same batch with similar dimensions was then mounted to expose a surface determined by the out-of-plane ($\| c$) and one of the in-plane ($\| a$) crystallographic directions. The crystal was photoexcited using midinfrared pump pulses generated using an optical parametric amplifier coupled to a difference frequency generation stage [32]. These pump pulses were polarized along the c axis and made to propagate through dispersive, optically polished NaCl plates before impinging on the sample. This yielded excitation pulses with the same spectral content but duration varying from 300 fs up to 2.5 ps.

Broadband terahertz probe pulses ($\approx$15–80 cm^{-1}), whose polarization was set to be parallel to the a axis, were focused on the sample and detected by electro-optical sampling after reflection in a 500-μm-thick ZnTe (110) crystal, yielding the photoinduced changes in the low-frequency complex reflection coefficient $\tilde{r}(\omega)$ as a function of pump-probe time delay [32].

In contrast to c-axis probe experiments, in all in-plane measurements reported here the penetration depth of the excitation pulses ($\approx$1 μm) was typically larger than that of the terahertz probe ($\approx$0.2–0.7 μm). Therefore, the probe pulses sampled a homogeneously excited volume and the transient optical properties could then be extracted directly, without the need to consider any pump-probe penetration depth mismatch in the data analysis. In this case, the complex refractive index of the photoexcited material, $\tilde{n}(\omega, \tau)$, was directly retrieved from the Fresnel relation, $\tilde{n}(\omega, \tau) = \frac{1-\tilde{r}(\omega,\tau)}{1+\tilde{r}(\omega,\tau)}$, and from this, the transient complex optical conductivity, $\tilde{\sigma}(\omega, \tau) = \frac{\omega}{4\pi i}[\tilde{n}(\omega, \tau)^2 - \varepsilon_\infty]$.

For consistency, all data were also analyzed with the same multilayer models used for the out-of-plane response, yielding very similar results [32].

III. RESULTS

As shown in Figs. 2(a) and 2(b), in the direction parallel to the Cu-O planes ($\| a$) the equilibrium normal state response of underdoped $YBa_2Cu_3O_{6+x}$ is that characteristic of a metal with Drude-like conductivity [29–31]: The real part, $\sigma_1(\omega)$, takes on large values, exceeding 4000 $\Omega^{-1}\,\text{cm}^{-1}$, and grows monotonically at low frequencies, approaching the DC value, while the imaginary part, $\sigma_2(\omega)$, exhibits a peak at finite frequency in correspondence with the carrier scattering rate, and becomes vanishingly small toward zero frequency. In addition, a collection of narrow absorption peaks is observed for $\omega \gtrsim 100\ \text{cm}^{-1}$, which are assigned to infrared-active phonons, only partially screened by the presence of mobile carriers.

In the superconducting state below T_C (blue curves), the low-frequency $\sigma_1(\omega)$ is strongly depleted for $\omega \lesssim 250\ \text{cm}^{-1}$, with a residual quasiparticle peak indicative of a d-wave superconducting gap [29–31]. Correspondingly, $\sigma_2(\omega)$ exhibits

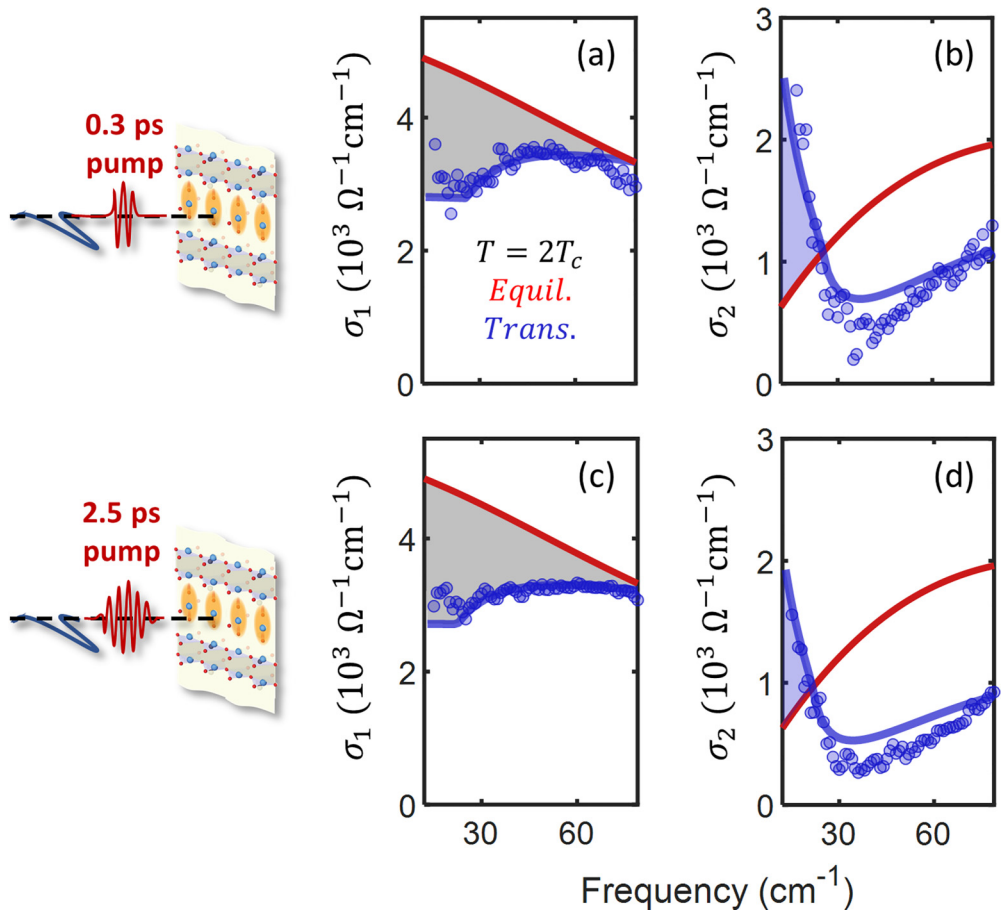

FIG. 3. Complex a-axis optical conductivity, $\sigma_1(\omega) + i\sigma_2(\omega)$, measured in $YBa_2Cu_3O_{6.48}$ at $T = 100$ K in equilibrium (red) and at one selected pump-probe time delay after photoexcitation (blue circles), corresponding to the peak of the coherent, superconducting-like response. We display data for different midinfrared pulse durations (shown on the left), all taken with the same pump fluence of $\sim$6.5 mJ/cm^2. Blue lines are fits to the spectra with the two-fluid model described in the text [32], featuring a superconducting component described by the Zimmermann model [35] and a second fluid made of uncondensed quasiparticles, described by a simple Drude model [36].

a $1/\omega$-like divergence at low frequencies, which is a signature of dissipationless transport [1].

The same type of equilibrium response has also been reported along the b crystallographic axis, albeit with higher values of the normal state conductivity [34]. However, the b-axis electrodynamics is dominated by the Cu-O chains, an element specific to cuprates of the $YBa_2Cu_3O_{6+x}$ family and absent in other compounds. Here, we focus our study exclusively on the response along the a axis.

In Figs. 2(c) and 2(d) we report representative results of our pump-probe experiment, in which we photoexcited $YBa_2Cu_3O_{6.48}$ at $T = 100\ \text{K} \simeq 2T_C$ with 300-fs-long, c-polarized midinfrared pulses tuned to be resonant with apical oxygen vibrations, and then probed the a-axis complex optical conductivity throughout its dynamical evolution. Note that unlike for c-axis probe measurements, the absence of a pump-probe penetration depth mismatch results in transient optical properties that are effectively uncertainty-free, and essentially independent of the model used to reconstruct them [see line thickness in Figs. 2(c) and 2(d)].

For the representative time delay shown here (blue curves), chosen to be at the peak of the response, we observe that $\sigma_1(\omega)$ reduces markedly from its equilibrium value, and develops a gap at low frequencies. Correspondingly, a $1/\omega$-like divergence appears in $\sigma_2(\omega)$ for $\omega \lesssim 30\ \text{cm}^{-1}$. Both of these features are suggestive of a superconducting-like response. However, while the photoinduced $\sigma_2(\omega)$ along the c axis (see Fig. 1) was also quantitatively very close to that measured at equilibrium below T_C, the transient response along the a axis is significantly smaller than the one measured in equilibrium when cooling below T_C. First, the photoinduced $\sigma_1(\omega)$ gap opens only at $\omega < 100\ \text{cm}^{-1}$, i.e., for frequencies much lower than the equilibrium below-T_C gap [29]. Second, $\sigma_2(\omega)$ also develops a divergence, but the value of $\lim_{\omega\to 0} \omega\sigma_2(\omega)$, which would be proportional to the superfluid density, is lower by at least a factor of 10 than the equilibrium value. Note also that we find no evidence of a residual Drude peak, which instead is observed in equilibrium.

In Fig. 3 we report representative spectra for different pump pulse durations. These data show no qualitative change, but only a reduction in the amplitude of the response compared with those in Fig. 2, presumably due to the lower peak electric field. All complex conductivity spectra show gapping in $\sigma_1(\omega)$ and the appearance of a low-frequency divergence

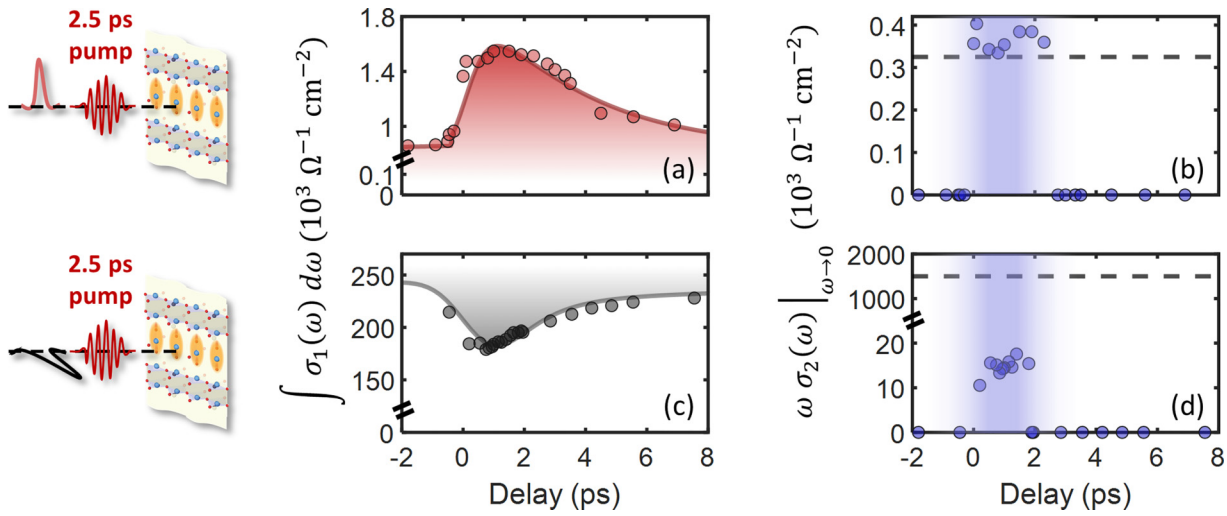

FIG. 4. Dynamical evolution of the transient spectral weight, $\int_{20\ \mathrm{cm}^{-1}}^{75\ \mathrm{cm}^{-1}} \sigma_1(\omega)\mathrm{d}\omega$ and of the coherent superconducting-like response, $\lim_{\omega\to 0}\omega\sigma_2(\omega)$, as a function of pump-probe time delay, measured in $YBa_2Cu_3O_{6.48}$ at $T = 100$ K upon excitation with 2.5-ps-long pulses, for both c- and a-axis probe polarizations (top and bottom panels, respectively). Data in (a) and (b) are replotted from Ref. [16], while those in (c) and (d) were acquired with a comparable pump fluence of $\sim$6.5 mJ/cm^2. Full lines in (a) and (c) are fits with a finite rise time and an exponential decay, while the dashed horizontal lines in (b) and (d) indicate the 10 K equilibrium values of the superfluid density. The blue shaded areas in the same panels represent the time delay window for which a finite coherent response was detected.

in $\sigma_2(\omega)$ following photoexcitation, which combined return a superconducting-like in-plane response (see Supplemental Material [32] for extended data sets).

IV. FITTING PROCEDURE

The dynamical evolution of dissipation and superconducting coherence is summarized by plotting the transient $\sigma_1(\omega)$ spectral weight loss $\int_{20\ \mathrm{cm}^{-1}}^{75\ \mathrm{cm}^{-1}} \sigma_1(\omega)\mathrm{d}\omega$ and the strength of the inductive coupling as $\lim_{\omega\to 0}\omega\sigma_2(\omega)$, extracted from the individual terahertz spectra measured at each time delay (see also analysis in Ref. [16]).

Figure 4 displays these two figures of merit for a representative data set, for both probe polarizations. Upon photoexcitation the $\sigma_1(\omega)$ spectral weight is enhanced along the c axis and reduced along the a axis, relaxing then on a timescale that clearly exceeds the pump pulse duration of 2.5 ps [Figs. 4(a) and 4(c)]. A different evolution is observed instead in $\lim_{\omega\to 0}\omega\sigma_2(\omega)$, which appears to be finite along both crystallographic axes only while the system is driven [blue shading in Figs. 4(b) and 4(d)]. A first implication of this result is that the transient conductivities from which the data in Fig. 4 were derived are well defined only down to $1/\tau \simeq 0.4$ THz, a cutoff that is below the low-frequency limit covered by our probe spectrum. Therefore, any ambiguity in the definition of the optical properties does not apply to our data with long pump pulses.

We also note that for the data set reported here, $\lim_{\omega\to 0}\omega\sigma_2(\omega)$ reaches, upon photoexcitation, values close to the c-axis equilibrium superfluid density measured at low temperature [dashed horizontal line in Fig. 4(b); see also Ref. [16]]. This is not found instead for the response along the planes, for which the transient "superfluid density" does not exceed a few percent of the equilibrium value [Fig. 4(d)].

We now turn to a more detailed analysis of transient optical properties and propose a model to fit the experimental data. In Ref. [16], it was discussed how the photoinduced response of the uncondensed quasiparticles and the "superfluid" were totally decoupled and showed up separately in the real and imaginary parts of the optical conductivity, respectively. The transient spectra were fitted with a Josephson plasma model in the presence of a residual Drude conductivity, with the formula $\tilde{\sigma}_a(\omega) = \frac{\omega_J^2}{4\pi}\frac{i}{\omega} + \tilde{\sigma}_D(\omega)$. Here, ω_J is the Josephson plasma frequency, while $\tilde{\sigma}_D(\omega)$ is an overdamped Drude term that reproduces the temperature-dependent flat offset found in $\sigma_1(\omega)$.

By comparing the photoinduced $\sigma_1(\omega)$ spectra with those measured at equilibrium at various temperatures and assuming rapid thermalization, we estimate the effective "heating" of uncondensed quasiparticles for various pump fluences and time delays. Maximum apparent temperature raises up to 150−200 K were extracted, in conjunction with a superconducting-like response in $\sigma_2(\omega)$, showing two completely decoupled dynamics of coherent and incoherent carriers.

This type of analysis is more complicated for the in-plane response. Along the planes the low-frequency $\sigma_2(\omega)$ is also dominated by the superconducting-like coherent response [see equilibrium spectra in Fig. 2(b)]. However, the reduction in $\sigma_1(\omega)$ found upon photoexcitation can be attributed to two effects. On the one hand, a gapping in the optical conductivity due to the presence of a superconducting condensate is expected. On the other, as can be seen by comparing the spectra at equilibrium measured at $T = 120$ K and $T = 200$ K in Fig. 2(a), an increase in the quasiparticle scattering rate with temperature also leads to a reduction in the low-frequency $\sigma_1(\omega)$ in our measurement range.

We fitted the in-plane complex conductivity of $YBa_2Cu_3O_{6.48}$ for various time delays and under different

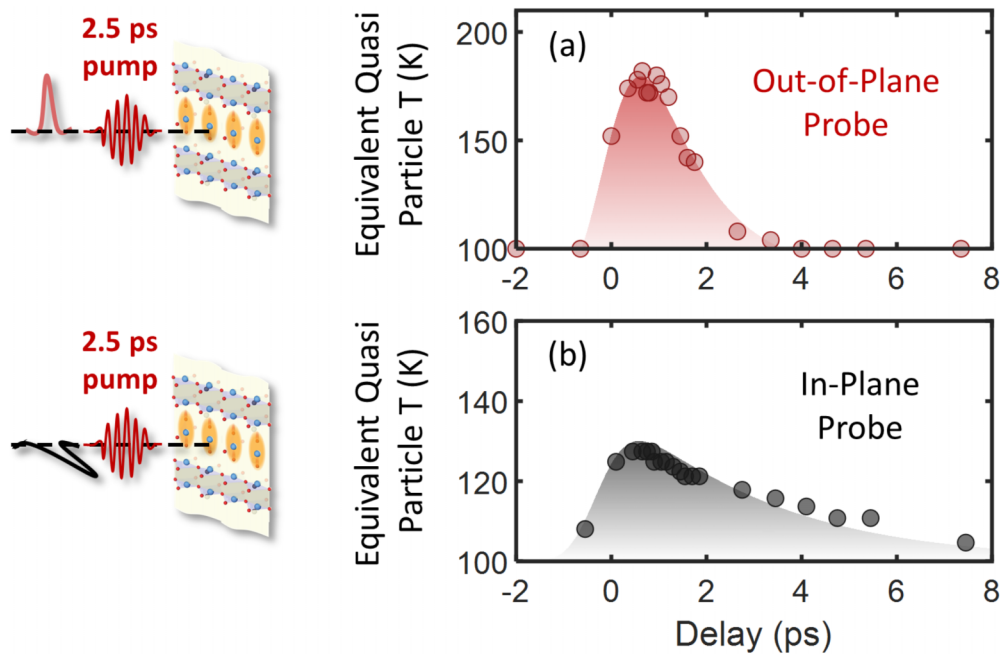

FIG. 5. Equivalent quasitemperatures for the uncondensed quasiparticles, extracted from fits to the complex optical conductivities measured in $YBa_2Cu_3O_{6.48}$ at a base temperature $T = 100$ K along both the c and the a axis, as described in the text [32]. The data refer to measurements taken in the same setup with 2.5 ps drive pulses and a pump fluence of $\sim$6.5 mJ/cm^2.

excitation conditions with a two-fluid model. The first fluid describes the response of a superconductor with the Zimmermann model [35], i.e., an extension of the Mattis-Bardeen model for superconductors of arbitrary purity, having the optical gap, 2Δ, as the fit parameter. The second fluid consists instead of unpaired residual quasiparticles [36], whose response is described by a Drude model with increased scattering rate, Γ, with respect to the equilibrium value, in order to account for carrier heating. In addition, to preserve the total number of carriers, we introduced a filling fraction parameter, f, so that the total fit formula is expressed as $\tilde{\sigma}_a(\omega) = f\tilde{\sigma}_{\mathrm{Zim}}(\omega, 2\Delta) + (1-f)\frac{\omega_P^2}{4\pi}\frac{1}{\Gamma - i\omega}$.

Examples of these fits are given for specific data sets in Fig. 3 (see also Supplemental Material [32]). The divergence found in $\sigma_2(\omega)$ at low frequencies is entirely due to the superconducting term, while the reduction in $\sigma_1(\omega)$ is partly to be attributed to quasiparticles heating, which appears as a rigid downward shift and broadening, and partly to the opening of the gap in $\tilde{\sigma}_{\mathrm{Zim}}$. Typical extracted parameters are $2\Delta \simeq 30$ cm^{-1}, $\Gamma \simeq 2\Gamma_{\mathrm{equil}}$, and f values around 20%.

This fitting procedure can be used to extract an equivalent temperature for the quasiparticles throughout the photoinduced dynamics in a similar way as reported in Ref. [16] for the out-of-plane response. Therein, by comparing the Drude parameters derived from the fits to the transient spectra with those performed on the conductivities at equilibrium for different temperatures (see also Fig. 2), we associated a quasitemperature with each out-of-equilibrium conductivity at different time delays and excitation conditions [32].

We follow here the same procedure, and plot an example of these "apparent" temperature dynamics in Fig. 5 for data sets acquired with 2.5 ps pump pulse duration and both probe polarizations, taken under the same excitation conditions. The peak value of this estimated quasitemperature is higher along the c axis than along the planes, while the relaxation dynamics appears slower in the direction parallel to the planes. These differences are presumably a result of the inadequate fitting procedure and of the comparison with the equilibrium spectra. It is not unlikely that other parameters, such as the carrier effective mass (incorporated in the plasma frequency, ω_P), are incorrectly assumed here to remain fixed during the dynamics.

V. CONCLUSIONS

We reported a study of the terahertz-frequency optical response of apical-oxygen-driven underdoped $YBa_2Cu_3O_{6+x}$ along the Cu-O planes, under the same excitation conditions for which an out-of-plane superconducting-like terahertz response and a transient magnetic field expulsion were observed. We measured the complex optical conductivity along the a axis, representative of the in-plane response, at $T = 100$ K $\simeq 2T_C$ for various excitation fluences and driving pulse durations, as a function of pump-probe time delay. Our findings are qualitatively similar to those expected for a transient superconducting response, with the opening of a gap in the real part of the optical conductivity, $\sigma_1(\omega)$, and the appearance of a low-frequency divergence in the imaginary part, $\sigma_2(\omega)$. By analyzing the dynamics of both the dissipative and the coherent parts of the photoinduced response we observed a very similar evolution of the same quantities measured along the c axis, finding that the coherent response in $\sigma_2(\omega)$ persists only as long as the drive is on. Using a two-fluid model we were then able to consistently fit the measured spectra and extract

physical parameters such as the equivalent quasitemperature of uncondensed quasiparticles.

Importantly, while the data reported along the c axis showed quantitative matching with the superconducting response measured at equilibrium below T_C, the in-plane response yields a transient optical gap and superfluid density lower than those observed at equilibrium.

These results, when combined with previous experiments, suggest that the driven pseudogap phase of underdoped $YBa_2Cu_3O_{6+x}$, exhibits a three-dimensional superconducting-like optical response, an observation that complements recent reports of an out-of-equilibrium Meissner effect. In this light, the explanations of magnetic field expulsion by large paramagnetism in a high-temperature cuprate with preexisting equilibrium short-range superconducting fluctuations appear less likely [37,38].

ACKNOWLEDGMENTS

We acknowledge support from the Deutsche Forschungsgemeinschaft (DFG, German Research Foundation) via the Cluster of Excellence CUI: Advanced Imaging of Matter (EXC 2056, project ID 390715994).

DATA AVAILABILITY

The data that support the findings of this article are openly available [33].

[1] D. N. Basov and T. Timusk, Electrodynamics of high-T_c superconductors, Rev. Mod. Phys. **77**, 721 (2005).

[2] C. C. Homes, T. Timusk, D. A. Bonn, R. Liang, and W. N. Hardy, Optical properties along the c-axis of $YBa_2Cu_3O_{6+x}$, for $x = 0.50 \rightarrow 0.95$. Evolution of the pseudogap, Physica C **254**, 265 (1995).

[3] C. C. Homes, T. Timusk, D. A. Bonn, R. Liang, and W. N. Hardy, Optical phonons polarized along the c axis of $YBa_2Cu_3O_{6+x}$, for $x = 0.5 \rightarrow 0.95$, Can. J. Phys. **73**, 663 (1995).

[4] D. N. Basov, S. I.Woods, A. S. Katz, E. J. Singley, R. C. Dynes, M. Xu, D. G. Hinks, C. C. Homes, and M. Strongin, Sum rules and interlayer conductivity of high-T_c cuprates, Science **283**, 49 (1999).

[5] D. van der Marel and A. Tsvetkov, Transverse optical plasmons in layered superconductors, Czech. J. Phys. **46**, 3165 (1996).

[6] D. van der Marel and A. A. Tsvetkov, Transverse-optical Josephson plasmons: Equations of motion, Phys. Rev. B **64**, 024530 (2001).

[7] H. Shibata and T. Yamada, Double Josephson plasma resonance in T^* phase $SmLa_{1-x}Sr_xCuO_{4-\delta}$, Phys. Rev. Lett. **81**, 3519 (1998).

[8] T. Kakeshita, S. Uchida, K. M. Kojima, S. Adachi, S. Tajima, B. Gorshunov, and M. Dressel, Transverse Josephson plasma mode in T^* cuprate superconductors, Phys. Rev. Lett. **86**, 4140 (2001).

[9] W. Hu, S. Kaiser, D. Nicoletti, C. R. Hunt, I. Gierz, M. C. Hoffmann, M. Le Tacon, T. Loew, B. Keimer, and A. Cavalleri, Optically enhanced coherent transport in $YBa_2Cu_3O_{6.5}$ by ultrafast redistribution of interlayer coupling, Nat. Mater. **13**, 705 (2014).

[10] S. Kaiser, C. R. Hunt, D. Nicoletti, W. Hu, I. Gierz, H. Y. Liu, M. Le Tacon, T. Loew, D. Haug, B. Keimer, and A. Cavalleri, Optically induced coherent transport far above T_c in underdoped $YBa_2Cu_3O_{6+x}$, Phys. Rev. B **89**, 184516 (2014).

[11] M. Först, A. Frano, S. Kaiser, R. Mankowsky, C. R. Hunt, J. J. Turner, G. L. Dakovski, M. P. Minitti, J. Robinson, T. Loew, M. Le Tacon, B. Keimer, J. P. Hill, A. Cavalleri, and S. S. Dhesi, Femtosecond x rays link melting of charge-density wave correlations and light-enhanced coherent transport in $YBa_2Cu_3O_{6.6}$, Phys. Rev. B **90**, 184514 (2014).

[12] R. Mankowsky, A. Subedi, M. Först, S. O. Mariager, M. Chollet, H. T. Lemke, J. S. Robinson, J. M. Glownia, M. P. Minitti, A. Frano, M. Fechner, N. A. Spaldin, T. Loew, B. Keimer, A. Georges, and A. Cavalleri, Nonlinear lattice dynamics as a basis for enhanced superconductivity in $YBa_2Cu_3O_{6.5}$, Nature (London) **516**, 71 (2014).

[13] R. Mankowsky, M. Först, T. Loew, J. Porras, B. Keimer, and A. Cavalleri, Coherent modulation of the $YBa_2Cu_3O_{6+x}$ atomic structure by displacive stimulated ionic Raman scattering, Phys. Rev. B **91**, 094308 (2015).

[14] C. R. Hunt, D. Nicoletti, S. Kaiser, D. Pröpper, T. Loew, J. Porras, B. Keimer, and A. Cavalleri, Dynamical decoherence of the light induced interlayer coupling in $YBa_2Cu_3O_{6+\delta}$, Phys. Rev. B **94**, 224303 (2016).

[15] B. Liu, M. Först, M. Fechner, D. Nicoletti, J. Porras, T. Loew, B. Keimer, and A. Cavalleri, Pump frequency resonances for light-induced incipient superconductivity in $YBa_2Cu_3O_{6.5}$, Phys. Rev. X **10**, 011053 (2020).

[16] A. Ribak, M. Buzzi, D. Nicoletti, R. Singla, Y. Liu, S. Nakata, B. Keimer, and A. Cavalleri, Two-fluid dynamics in driven $YBa_2Cu_3O_{6.48}$, Phys. Rev. B **107**, 104508 (2023).

[17] D. Nicoletti, E. Casandruc, Y. Laplace, V. Khanna, C. R. Hunt, S. Kaiser, S. S. Dhesi, G. D. Gu, J. P. Hill, and A. Cavalleri, Optically induced superconductivity in striped $La_{2-x}Ba_xCuO_4$ by polarization-selective excitation in the near infrared, Phys. Rev. B **90**, 100503(R) (2014).

[18] E. Casandruc, D. Nicoletti, S. Rajasekaran, Y. Laplace, V. Khanna, G. D. Gu, J. P. Hill, and A. Cavalleri, Wavelength-dependent optical enhancement of superconducting interlayer coupling in $La_{1.885}Ba_{0.115}CuO_4$, Phys. Rev. B **91**, 174502 (2015).

[19] D. Nicoletti, D. Fu, O. Mehio, S. Moore, A. S. Disa, G. D. Gu, and A. Cavalleri, Magnetic-field tuning of light-induced superconductivity in striped $La_{2-x}Ba_xCuO_4$, Phys. Rev. Lett. **121**, 267003 (2018).

[20] S. Fava, G. De Vecchi, G. Jotzu, M. Buzzi, T. Gebert, Y. Liu, B. Keimer, and A. Cavalleri, Magnetic field expulsion in optically driven $YBa_2Cu_3O_{6.48}$, Nature (London) **632**, 75 (2024).

[21] A. von Hoegen, M. Fechner, M. Först, N. Taherian, E. Rowe, A. Ribak, J. Porras, B. Keimer, M. Michael, E. Demler, and A. Cavalleri, Amplification of superconducting fluctuations in driven $YBa_2Cu_3O_{6+x}$, Phys. Rev. X **12**, 031008 (2022).

[22] M. H. Michael, A. von Hoegen, M. Fechner, M. Först, A. Cavalleri, and E. Demler, Parametric resonance of Josephson plasma waves: A theory for optically amplified interlayer

superconductivity in $YBa_2Cu_3O_{6+x}$, Phys. Rev. B **102**, 174505 (2020).

[23] N. Taherian, M. Först, A. Liu, M. Fechner, D. Pavicevic, A. von Hoegen, E. Rowe, Y. Liu, S. Nakata, B. Keimer, E. Demler, M. H. Michael, and A. Cavalleri, Probing amplified Josephson plasmons in $YBa_2Cu_3O_{6+x}$ by multidimensional spectroscopy, npj Quantum Mater. **10**, 54 (2025).

[24] S. J. Zhang, Z. X. Wang, H. Xiang, X. Yao, Q. M. Liu, L. Y. Shi, T. Lin, T. Dong, D. Wu, and N. L. Wang, Photoinduced nonequilibrium response in underdoped $YBa_2Cu_3O_{6+x}$ probed by time-resolved terahertz spectroscopy, Phys. Rev. X **10**, 011056 (2020).

[25] K. Katsumi, M. Nishida, S. Kaiser, S. Miyasaka, S. Tajima, and R. Shimano, Near-infrared light-induced superconducting-like state in underdoped $YBa_2Cu_3O_y$ studied by c-axis terahertz third-harmonic generation, Phys. Rev. B **107**, 214506 (2023).

[26] J. S. Dodge, L. Lopez, and D. G. Sahota, Optical saturation produces spurious evidence for photoinduced superconductivity in K_3C_{60}, Phys. Rev. Lett. **130**, 146002 (2023).

[27] M. Buzzi, D. Nicoletti, E. Rowe, E. Wang, and A. Cavalleri, Comment on arXiv:2210.01114: Optical Saturation Produces Spurious Evidence for Photoinduced Superconductivity in K_3C_{60}, arXiv:2303.10169.

[28] S. J. Zhang, X. Y. Zhou, S. X. Xu, Q. Wu, L. Yue, Q. M. Liu, T. C. Hu, R. S. Li, J. Y. Yuan, C. C. Homes, G. D. Gu, T. Dong, and N. L. Wang, Light-induced melting of competing stripe orders without introducing superconductivity in $La_{2-x}Ba_xCuO_4$, Phys. Rev. X **14**, 011036 (2024).

[29] Y. S. Lee, K. Segawa, Z. Q. Li, W. J. Padilla, M. Dumm, S. V. Dordevic, C. C. Homes, Y. Ando, and D. N. Basov, Electrodynamics of the nodal metal state in weakly doped high-T_c cuprates, Phys. Rev. B **72**, 054529 (2005).

[30] Y.-S. Lee, K. Segawa, Y. Ando, and D. N. Basov, Coherence and superconductivity in coupled one-dimensional chains: A case study of $YBa_2Cu_3O_y$, Phys. Rev. Lett. **94**, 137004 (2005).

[31] J. Hwang, J. Yang, T. Timusk, S. G. Sharapov, J. P. Carbotte, D. A. Bonn, R. Liang, and W. N. Hardy, a-axis optical conductivity of detwinned ortho-II $YBa_2Cu_3O_{6.50}$, Phys. Rev. B **73**, 014508 (2006).

[32] See Supplemental Material at http://link.aps.org/supplemental/10.1103/2m3d-s3j9 for sample growth and characterization, equilibrium optical properties, pump-probe setup and data acquisition, determination of the transient optical properties, fitting models, extracted parameters, and extended data sets, which includes Refs. [15,16,26,29–31,35,36,39–43].

[33] M. Rosenberg, D. Nicoletti, M. Buzzi, A. Iudica, C. Putzke, Y. Liu, B. Keimer, and A. Cavalleri, Source data for Figs. 1–5 can be found at D. Nicoletti 2025, Signatures of three-dimensional photoinduced superconductivity in $YBa_2Cu_3O_{6.48}$ (2025), Edmond, https://doi.org/10.17617/3.U3DF60.

[34] Y.-S. Lee, K. Segawa, Y. Ando, and D. N. Basov, Quasiparticle dynamics and in-plane anisotropy in $YBa_2Cu_3O_y$ near the onset of superconductivity, Phys. Rev. B **70**, 014518 (2004).

[35] W. Zimmermann, E. H. Brandt, M. Bauer, E. Seider, and L. Genzel, Optical conductivity of BCS superconductors with arbitrary purity, Phys. C (Amsterdam, Neth.) **183**, 99 (1991).

[36] Z. Tagay, F. Mahmood, A. Legros, T. Sarkar, R. L. Greene, and N. P. Armitage, BCS d-wave behavior in the terahertz electrodynamic response of electron-doped cuprate superconductors, Phys. Rev. B **104**, 064501 (2021).

[37] M. H. Michael, D. De Santis, E. A. Demler, and P. A. Lee, Giant Dynamical Paramagnetism in the driven pseudogap phase of $YBa_2Cu_3O_{6+x}$, arXiv:2410.12919.

[38] M. H. Michael, E. A. Demler, and P. A. Lee, Parametrically amplified Josephson plasma waves in $YBa_2Cu_3O_{6+x}$: Evidence for local superconducting fluctuations up to the pseudogap temperature T^*, arXiv:2505.03358.

[39] J. T. Kindt and C. A. Schmuttenmaer, Theory for determination of the low-frequency time-dependent response function in liquids using time-resolved terahertz pulse spectroscopy, J. Chem. Phys. **110**, 8589 (1999).

[40] D. van der Marel, H. J. A. Molegraaf, J. Zaanen, Z. Nussinov, F. Carbone, A. Damascelli, H. Eisaki, M. Greven, P. H. Kes, and M. Li, Quantum critical behaviour in a high-T_c superconductor, Nature (London) **425**, 271 (2003).

[41] L. Lopez, D. G. Sahota, and J. S. Dodge, Nonlinear photoconductivity in pump-probe spectroscopy. I. Optical coefficients, arXiv:2410.21496.

[42] M. Born and E. Wolf, *Principles of Optics*, 7th ed. (Cambridge University Press, Cambridge, 1999).

[43] A. B. Kuzmenko, D. van der Marel, F. Carbone, and F. Marsiglio, Model-independent sum rule analysis based on limited-range spectral data, New J. Phys. **9**, 229 (2007).